Proceedings of the 2002 IEEE/RSJ
Intl. Conference on Intelligent Robots and Systems
EPFL, Lausanne, Switzerland • October 2002

Screw bondgraph contact dynamics

Martijn Visser, Stefano Stramigioli and Cock Heemskerk

Fokker Space BV, Leiden, the Netherlands, m.visser@fokkerspace.nl, c.heemskerk@fokkerspace.nl
Drebbel Institute, University of Twente, Enschede, the Netherlands, s.stramigioli@ieee.org

Abstract

This paper presents an elegant contact dynamics model in screw bondgraph form. It can model the contact between any two objects of finite curvature. It does so by defining a Gauss frame on the surfaces of both objects in the points that are closest to each other. Then it describes how the Gauss frames move as the objects move relative to each other. This is called the contact kinematics. The contact kinematics detect when two objects touch, then describe how they roll and slide over and along each other, and then detect when they get loose again. With the contact kinematics a dynamic screw bondgraph model is build. This dynamics model is verified in two simulations. The first simulation shows two objects of nontrivial curvature, eggs, rolling over each other. The second shows a robotic hand manipulating an object.

1 Introduction

1.1 Twin Arm Robot

Fokker Space is prime contractor for the European Robotic Arm (ERA) [11]. ERA is a 12 m long, 600 kg arm that can handle payloads of upto 8000 kg. It will help in the assembly and maintenance of the Russian segment of the International Space Station (ISS). It is not intended and suitable for smaller, more human-scale, maintenance and repair tasks. Those tasks are now performed by cosmonauts in Extra Vehicular Activity (EVA) which is both dangerous and costly. For this reason Fokker Space is researching a small, relatively autonomous robot called Twin Arm Robot (TAR) [10]. TAR is to replace and assist cosmonauts in EVA. The TAR has two 7 DOF arms and two 3 finger, 12 DOF Compact Dexterous Gripper's (CDG) as hands. Figure 1 shows a prototype of a CDG finger.

Most tasks that the TAR will have to perform, involve contact between the robot and the environment. This holds not only for TAR but for most useful tasks that robots can perform in general. The CDG for example can grasp an object, and manipulate the object between its fingers. To understand the contact, and to simulate the contact we need a contact model. A contact model can for example be used to study different grasping and manipulation schemes.

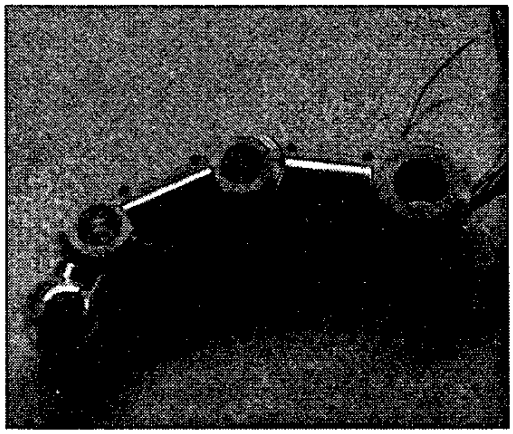

Figure 1: *Prototype of Compact Dexterous Gripper finger*

1.2 Existing contact models

In literature different contact models can be found. Most of them assume that the contacting objects have very specific shapes like for example the contact models described in [4] and [6]: [4] which is used inside the ERA Simulation Facility (ESF), can only model the contact between points and planes, while Ma [6] assumes that the surfaces of the objects are linear or quadratic. Montana [1] on the other hand only assumes that the objects have finite curvature, which means that the objects may not have infinetely sharp edges. This is the most general model because in reality edges are never infinitely sharp. Montana's model however has the following two limitations.

First it assumes that the objects are in contact. It cannot detect contact while [4] and [6] can. For the points and planes in [4] the contact detection is trivial and [6] uses a numerical optimization algorithm to detect contact. Secondly Montana's model is only a kinematic model while [4] and [6] are fully dynamic models. [4] treats the objects as infinitely stiff but [6] takes the finite object stiff-

ness into account. Both contact detection and dynamics are essenstial in creating controllers for dexterous robots performing contact tasks.

This paper generalizes Montana's contact kinematics so that it can also detect contact, and then uses the generalized contact kinematics in a dynamic screw bondgraph model. The rest of this paper is organized as follows. First in section 2 some background on twists and wrenches and geometry of surfaces is reviewed. In section 3 the contact kinematics are generalized to include the contact detection. In 4 the contact kinematics are used in a dynamic screw bondgraph model. In section 5 the dynamics model is verified in simulations. Finally in section 6 the conclusions are presented.

2 Background

2.1 Twists and wrenches

Let $SE(3)$ be the special Euclidean Lie group. Let $H_2^1 \in SE(3)$ be the pose that relates frame 2 to frame 1. H_2^1 is both a coordinate transformation and a motion. It is a coordinate transformation that transforms coordinates of points p and vectors v from frame 2 to frame 1. It is a motion that moves frame 1 to frame 2. p_2^1 are the coordinates of the origin of frame 2 in frame 1. The columns of R_2^1 are the coordinates of the axes of frame 2 in frame 1.

$$H_2^1 = \begin{bmatrix} R_2^1 & p_2^1 \\ 0 & 1 \end{bmatrix} \tag{1}$$

Let $se(3)$ be the special Euclidean Lie algebra associated to $SE(3)$. Let T_3^{12} be the twist of frame 3 relative to frame 2 expressed in frame 1 with angular part ω_3^{12} and linear part v_3^{12}. v_3^{12} is the velocity of a point that is fixed in frame 3 but momentarily coincides with the origin of frame 1 relative to frame 2. This is not the same as the velocity of the origin of frame 3!

$$T_3^{12} = \begin{bmatrix} \omega_3^{12} \\ v_3^{12} \end{bmatrix} \tag{2}$$

The big advantage of twists over velocities is that each point on the same rigid body can be described with the same twist but not the same velocity. If frame 1 is the same as frame 2 then T_3^{22} is called the world twist. If frame 1 is the same as frame 3 then T_3^{32} is called the body twist. The relation between the world and body twists on the one hand, and the time derivative of the pose is as follows.

$$T_3^{22} = \dot{H}_3^2 H_2^3 \quad \text{and} \quad T_3^{32} = H_2^3 \dot{H}_3^2 \tag{3}$$

The adjoint map $Ad_{H_2^1}$ transforms twists from frame 2 to frame 1, where

$$Ad_{H_2^1} = \begin{bmatrix} R_2^1 & 0 \\ p_2^1 R_2^1 & R_2^1 \end{bmatrix} \tag{4}$$

Its transpose transforms wrenches from frame 1 to frame 2. For more information on twists and wrenches see [7].

2.2 Geometry of surfaces

Consider S be the surface of an object embedded in 3 dimensional Euclidean space $E(3)$. Let the surface be oriented in such a way that the normal is pointing away from the object. Let $c(q)$ be an orthogonal (not orthonormal) parameterization of the surface around a point $p \in S$, with local coordinates $q = (u, v)$ and that is compatible with the orientation. Such a parameterization always exists in a neighborhood around p. For a proof see [5]. Then a coordinate frame can be attached to p in the following way: the X axis of the coordinate frame is the unit vector pointing in the direction of the first coordinate u of the parameterization c. In the same way the Y axis is the unit vector pointing in the direction of the second coordinate v. The Z axis is the unit normal vector N.

$$x = \frac{c_u}{\|c_u\|}, \quad y = \frac{c_v}{\|c_v\|} \quad \text{and} \quad z = \frac{c_u}{\|c_u\|} \times \frac{c_v}{\|c_v\|} \tag{5}$$

where the notation c_u means $\frac{\partial c}{\partial u}$. This frame is called the normalized Gauss frame $H(q)$.

$$H(q) = \begin{bmatrix} x & y & z & c \\ & 0 & & 1 \end{bmatrix} \tag{6}$$

Because the surface is embedded in $E(3)$ it inherits a Riemannian metric. From this metric follow the first and the second fundamental forms and the Christoffel symbols. The first fundamental form is a measure for the length of a vector tangent to the surface. Montana [1] uses the first fundamental form to define the metric matrix M. Because the parameterization is orthogonal the metric matrix is diagonal.

$$M = \begin{bmatrix} \|c_u\| & 0 \\ 0 & \|c_v\| \end{bmatrix} \tag{7}$$

The second fundamental form is a measure for the curvature of the surface along a tangent vector. Montana uses the second fundamental form to define the curvature matrix K.

$$K = \begin{bmatrix} x^T \\ y^T \end{bmatrix} \begin{bmatrix} \frac{z_u}{\|c_u\|} & \frac{z_v}{\|c_v\|} \end{bmatrix} \tag{8}$$

Finally Montana defines the torsion vector T that is a measure for how the Gauss frame twists as it moves

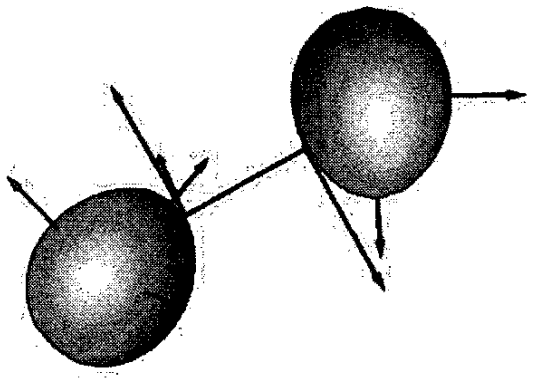

Figure 2: Shortest distance between two objects and their Gauss frames

across the surface. The torsion vector is related to the Christoffel symbols.

$$T = y^T \begin{bmatrix} \frac{x_u}{\|c_u\|} & \frac{x_v}{\|c_v\|} \end{bmatrix} \quad (9)$$

Montana calls M, K and T tensors but they are not really tensors as is explained in [12]. The metric, curvature and torsion together fully describe the geometry of the surface. They will be used to derive the contact kinematics. For more information on the geometry of surfaces see [5].

3 Contact kinematics

Montana [1] first derived the contact kinematics for the case when two objects are in contact. For a coordinate-free, intrinsic derivation see [12]. Here we will generalize the kinematics to the case where the two objects need not be in contact.

Consider two objects 1 and 2 with surfaces S_1 and S_2. The shortest distance between the surfaces of two objects is along a line that is perpendicular to both surfaces. Lets call the points where this line intersects the surfaces p_1 and p_2 and their distance d. Let $c_1(u_1, v_1)$ and $c_2(u_2, v_2)$ be parameterizations of S_1 and S_2 around p_1 and p_2, that satisfy the conditions in section 2.2.

We define the following frames: frame W is the world frame that is fixed. Frames O_1 and O_2 are the object frames that are fixed relative to the objects. The object frames can for example be chosen in the centers of gravity with their axes along the principal axes of inertia. C_1 and C_2 are the contact frames, which are the normalized Gauss frames of c_1 and c_2 in p_1 and p_2, and move with the contact point.

The relative pose of objects 1 and 2 that are in contact, is uniquely defined by the six contact coordinates: the two pairs of local coordinates (u_1, v_1) and (u_2, v_2), the relative angle α and the relative distance d. The relative angle α is the angle from x_1 to x_2 measured about z_1. Of course the number of coordinates necessary to describe the relative pose of two objects is 6 because the dimension of $SE(3)$ which is the space of relative poses is 6.

By definition the pose of the contact frames relative to the object frames H_C^O are given by (6). Using (3) we compute their body twists T_C^{CO}. This is were the properties introduced in section 2.2 come in useful. Writing out and substituting (7) through (9) we get for the angular part (again see [1])

$$\begin{bmatrix} (\omega_C^{CO})_y \\ -(\omega_C^{CO})_x \end{bmatrix} = KM\dot{q} \quad \text{and} \quad (\omega_C^{CO})_z = TM\dot{q} \quad (10)$$

where $q = (u, v)$, and for the linear part

$$\begin{bmatrix} (v_C^{CO})_x \\ (v_C^{CO})_y \end{bmatrix} = M\dot{q} \quad \text{and} \quad (v_C^{CO})_z = 0 \quad (11)$$

By definition the contact frames C_1 and C_2 have common Z axes pointing towards eachother's origin and therefore

$$H_{C_2}^{C_1} = \begin{bmatrix} R_{C_2}^{C_1} & p_{C_2}^{C_1} \\ 0 & 1 \end{bmatrix} \quad (12)$$

with

$$p_{C_2}^{C_1} = \begin{bmatrix} 0 \\ 0 \\ d \end{bmatrix} \quad \text{and} \quad R_{C_2}^{C_1} = \begin{bmatrix} R & 0 \\ 0 & -1 \end{bmatrix} \quad (13)$$

where

$$R = \begin{bmatrix} cos(\alpha) & -sin(\alpha) \\ -sin(\alpha) & cos(\alpha) \end{bmatrix} \quad (14)$$

Using (3) we compute the body twist. As expected it has only an angular and linear component about and along the common Z axis.

$$T_{C_2}^{C_2C_1} = \begin{bmatrix} \omega_{C_2}^{C_2C_1} \\ v_{C_2}^{C_2C_1} \end{bmatrix} \quad \omega_{C_2}^{C_2C_1} = \begin{bmatrix} 0 \\ 0 \\ \dot{\alpha} \end{bmatrix} \quad v_{C_2}^{C_2C_1} = \begin{bmatrix} 0 \\ 0 \\ \dot{d} \end{bmatrix} \quad (15)$$

To compute the twist of O_2 relative to O_1 we go from O_1 to C_1 to C_2 to O_2. Expressing all the twists in the chain in C_2 we can easily sum them

$$T_{O_2}^{C_2O_1} = T_{O_2}^{C_2C_2} + T_{C_2}^{C_2C_1} + T_{C_1}^{C_2O_1} \quad (16)$$

Using (4) and the fact that the twist of C_2 relative to C_1 is the same as the twist of O_2 relative to C_2 but with opposite sign, we get

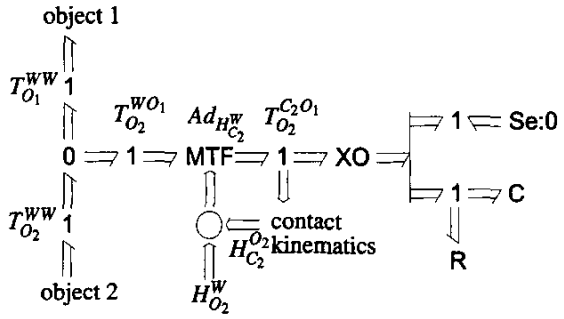

Figure 3: Contact dynamics in screw bondgraph form

$$T_{O_2}^{C_2O_1} = -T_{C_2}^{C_2O_2} + T_{C_2}^{C_2C_1} + Ad_{H_{C_1}^{C_2}} T_{C_1}^{C_1O_1} \tag{17}$$

Using (4) and substituting (10) through (15) we get after laborious rearranging for the rates of the contact coordinates as a function of the body twist of O_2 relative to O_1

$$\dot{q}_1 = M_1^{-1} R \left(K_2 \left(dRK_1R + I\right) + RK_1R\right)^{-1} \left(\begin{bmatrix} -\omega_y \\ \omega_x \end{bmatrix} + K_2 \begin{bmatrix} v_x \\ v_y \end{bmatrix} \right) \tag{18}$$

$$\dot{q}_2 = M_2^{-1} \left(\left(dRK_1R + I\right)K2 + RK_1R\right)^{-1} \left(\left(dRK_1R + I\right) \begin{bmatrix} -\omega_y \\ \omega_x \end{bmatrix} + RK_1R \begin{bmatrix} v_x \\ v_y \end{bmatrix} \right) \tag{19}$$

$$\dot{\alpha} = \omega_z + T_1 M_1 \dot{q}_1 + T_2 M_2 \dot{q}_2 \tag{20}$$

$$\dot{d} = v_z \tag{21}$$

where M_i, K_i, T_i and q_i are the metric, curvature, torsion and local coordinates of object i.

Equations (18) through (21) are the generalized contact kinematics. They are very similar to Montana's contact kinematics for two objects that are in contact. The only difference is the term $(dRK_1R + I)$ to account for the distance d. If $d = 0$, that is if the objects are in contact, the generalized contact kinematics reduce to Montana's contact kinematics [1].

Now we will extend the generalized contact kinematics to a dynamic screw bondgraph model.

4 Contact dynamics

In figure 3 we see the dynamic screw bondgraph contact dynamics model. For a background on screw bondgraphs see [9]. The bondgraph model has two power ports connected to two objects, and one input, namely the object frame of one of the objects, for example $H_{O_2}^W$. The power-conjugate variables of the ports are the world twists of both objects $T_{O_1}^{WW}$ and $T_{O_2}^{WW}$ and their respective wrenches.

The twists are subtracted to get their relative twist $T_{O_2}^{WO_1}$. Then, using the using adjoint map (4) the relative twist is expressed in one of the contact frames to get $T_{O_2}^{C_2O_1}$. For this we need $H_{C_2}^W$ which we build from $H_{O_2}^W$ and $H_{C_2}^{O_2}$.

$T_{O_2}^{C_2O_1}$ is input to the contact kinematics, which compute the rates of the contact coordinates, that are integrated to get the contact coordinates themselves. XO is a switched junction: depending on whether there is contact (when the distance, which is the sixth contact coordinate, is greater than zero), it switches the power flow to the rest of the model on or off.

If there is contact, so the model is switched on, the different DOF's of $T_{O_2}^{C_2O_1}$ are split into free and constrained DOF's. For rolling contact ω_x and ω_y are free and the other DOF's are constrained. For sliding contact ω_z, v_x and v_y are free and the other DOF's are constrained. For rolling and sliding contact all DOF's except v_z are free.

The free DOF's are connected to an effort source Se of zero (zero torque or force). The constrained DOF's are connected to springs C and dampers R. The stiffness of the spring and damping of the damper depend on material properties of both objects, a relation for which can be found in [6]. If the springs are pressed the object is slightly deformed. We have assumed that these deformations are small relative to the size of the object, so that the shape of the objects given by the parameterization, remains approximately the same.

Because a bondgraph model can be automatically translated into causal equations, it can be simulated easily. In the next section we will show some simulations.

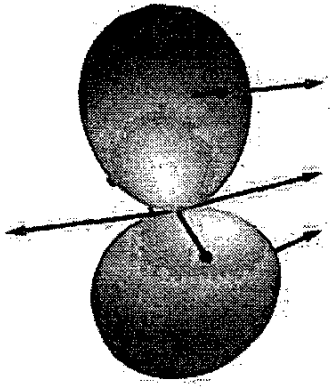

Figure 4: Simulation of two eggs rolling over each other

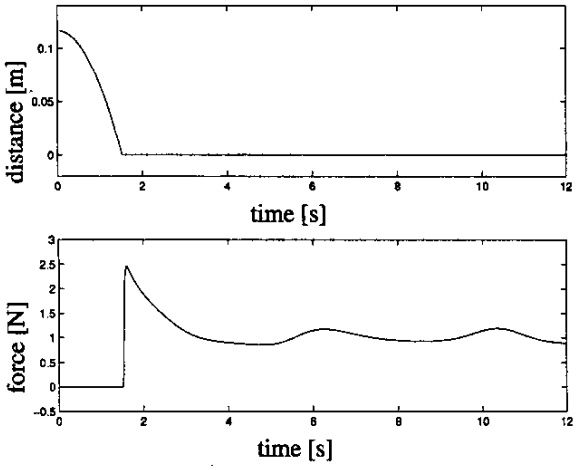

Figure 5: Distance and force between two eggs

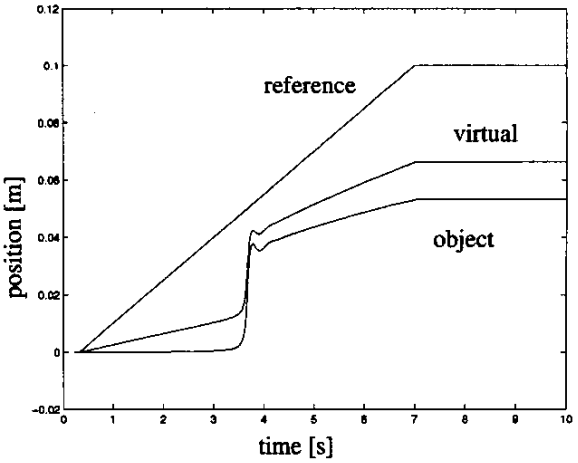

Figure 7: The object follows the virtual object which follows the reference

5 Simulations

In order to verify our dynamic model we simulate two objects rolling over each other. For the objects we take Cartesian ovals because they have a nontrivial curvature. A Cartesian oval is a special kind of oval which looks like an egg. Just as a regular oval is the collection of points where the sum of the distances to its two focal points is constant, a Cartesian oval is the collection of points where the sum of the distance to one focal point plus twice the distance to the other focal point is constant. In figure 4 we see the two eggs, their object frames and their Gauss frames. In figure 5 we see the distance and the force between them as a function of the time. When the distance becomes zeros there is contact and we see an impact in the force. The shape of the rest of the force is because of the shape of the eggs: the "humps" are when one of the eggs rolls over its top.

As an application we show a simulation of the CDG manipulating an object, in this case a sphere. The fingers are the same as the one in figure 1. In figure 6 we see three frames: the first one is the reference frame, the third the object frame and the second the virtual object frame which exists only in the controller. The used controller is a special form of impedance control. For more information on the controller see [9]. The hand has to make the object follow the reference by rolling it between its fingers and without dropping it. In figure 7 the reference position, object position and virtual object position are plotted as a function of the time. In the beginning the fingers turn, then they move with the object in the right direction and finally stop as the reference moves outside the reach of the hand.

The simulations have been performed with 20-sim [13], which is a powerful modeling and simulation package which supports bondgraphs.

6 Conclusions

In this paper the contact kinematics as first derived by Montana [1] have been generalized to include the case when the objects are not (yet) in contact. They can model contact between any two objects of finite positive relative curvature. They can detect when two objects touch, how they roll and slide over eachother and when they come loose again.

The generalized contact kinematics have been used in a dynamic bondgraph model. When the objects are in contact certain DOF's are constrained and the others are free. Depending on which DOF's are constrained the objects roll and / or slide over each other. The constrained DOF's are modeled by a spring and a damper in parallel, the stiffness and damping of which depend on material properties.

The contact dynamics model has been verified with a simulation of two objects of nontrivial curvature (Cartesian ovals or eggs) rolling over each other. An example of an application has been given for a hand that manipulates an object, by rolling the object between its fingers, using a special form of impedance control.

In the future research we will extend the model to include friction. That is rolling contact which above a certain force also becomes sliding contact. We will use this model to study different grasping and manipulation schemes, an example of which has already been given in section 5.

7 Acknowledgements

The contribution of Martijn Visser has been partly sponsered by Fokker Space BV. The contribution of Stefano Stramigioli has been sponsered by the GeoPlex project.

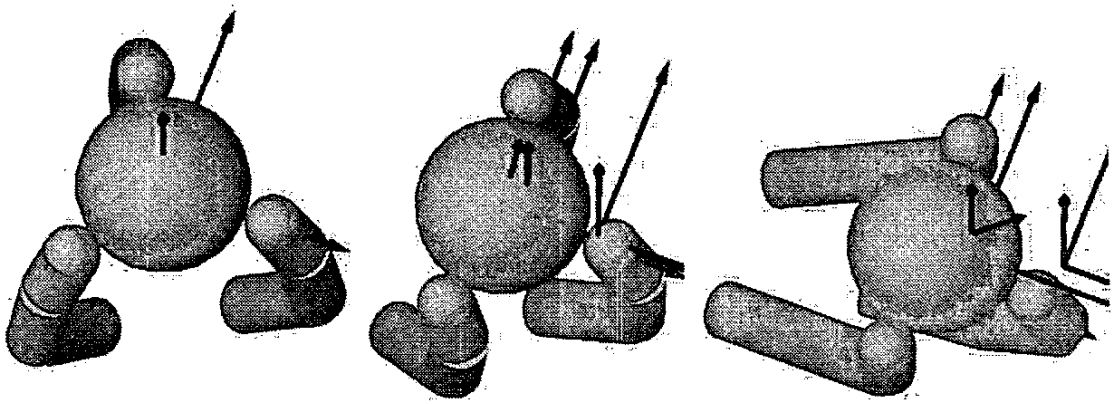

Figure 6: Robotic hand manipulating an object

References

[1] David J. Montana: "The kinematics of contact and grasp", *International Journal of Robotics Research* vol. 7 no. 3 pp. 17–32, June 1988

[2] David J. Montana: "The kinematics of contact with compliance", *Proceedings of the IEEE International Conference on Robotics and Automation* pp. 770–774, 1989

[3] Arlene B.A. Cole, John E. Hauser and S. Shankar Sastry: "Kinematics and control of multi-fingered hands with rolling contact", *IEEE Transactions on Automatic Control* vol. 34 no. 4 pp. 398–404, April 1989

[4] Marcel Ellenbroek: *"On the fast simulation of the multibody dynamics of flexible space structures: the recursive thought"*, PhD thesis from Twente University, Enschede, the Netherlands, November 1994

[5] M.P. do Carmo: *"Differential geometry of curves and surfaces"*, Englewood Cliffs, Prentice Hall, 1976

[6] Ou Ma: "Contact dynamics modeling for the simulation of the space station manipulators handling payloads", *submitted to the IEEE International Conference on Robotics and Automation*, Nagoya, Japan, May 1995

[7] Stefano Stramigioli and Herman Bruyninckx: "Geometry and screw theory for robotics", *tutorial from IEEE International Conference on Robotics and Automation*, Seoul, Korea, 2001

[8] Stefano Stramigioli: "A novel impedance grasping strategy based on the virtual object concept", *IEEE Mediterranean Conference on Control and Systems*, Alghero, Italy, June 1998

[9] Stefano Stramigioli: "Modeling and IPC control of interactive mechanical systems: a coordinate-free approach", Springer, Londen, 2001

[10] Cock J.M. Heemskerk and Martijn Visser: "TAR: a twin arm robot for dexterous assembly and maintenance tasks on ISS", *Proceedings of the ESA Workshop on Advanced Space Technologies for Robotics and Automation*, Noordwijk, the Netherlands, December 2000

[11] R. Boumans and Cock Heemskerk: "European Robotic Arm for the International Space Station", *Robotics and Autonomous Systems* vol. 23 pp. 17 - 27, 1998

[12] Vincent Duindam and Stefano Stramigioli: "Coordinate free derivation of contact kinematics", *submitted to the IEEE International Conference on Intelligent Robots and Systems*, Lausanne, Switzerland, October 2002

[13] http://www.20sim.com/